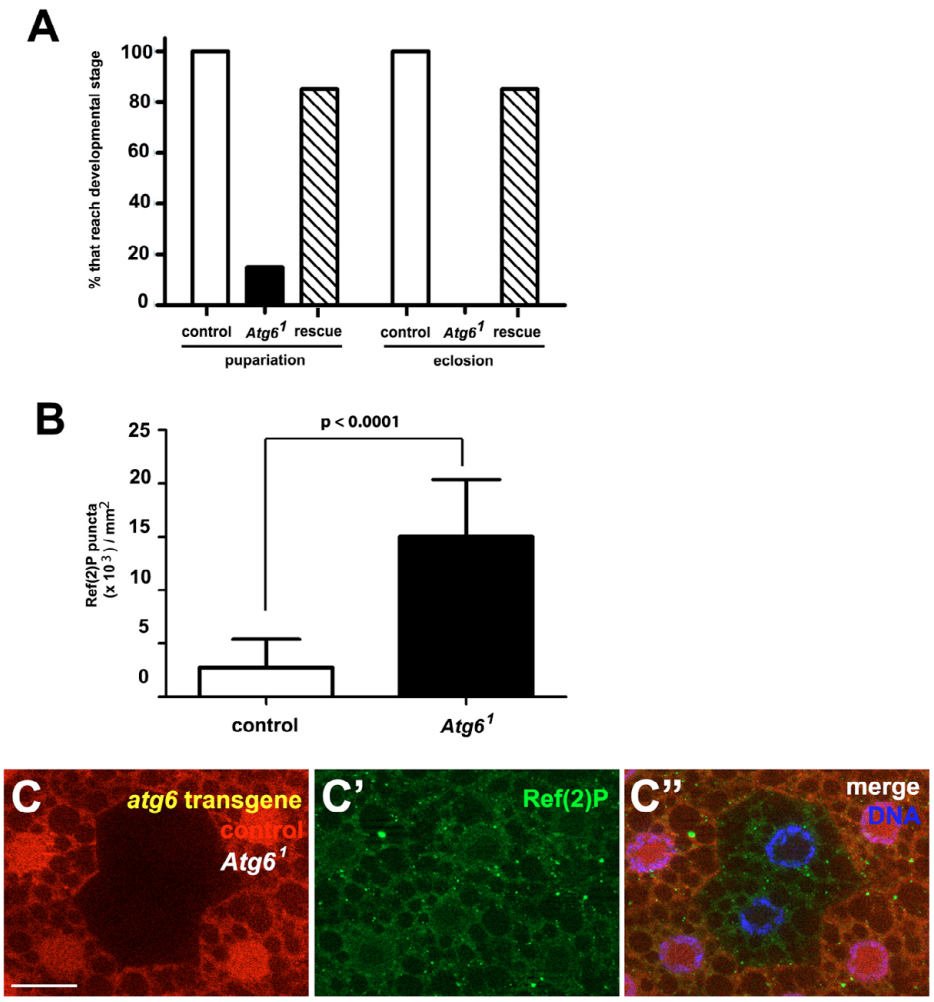

Fig. S1 *Atg6* is required for development and autophagy. (**A**) *Atg6* is required for development, as homozygous *Atg6* mutant animals die during development. Most homozygous *Atg6*^{1} animal lethality occurs prior to puparium formation, and lethality can be rescued by expressing an *atg6* transgene ubiquitously in the whole animal. (**B**) Quantification of Ref(2)P (fly p62) puncta in control and homozygous *Atg6*^{1} mutant fat body cells as in Fig. 1G. A two-tailed *t*-test was used for statistical analysis, and the *P*-value relative to control was 5.07×10^{-9}. The error bars represent s.d. (**C-C''**) Ref(2)P aggregates did not accumulate *Atg6*^{1}mutant clone cells (mCherry negative) expressing a myc-tagged *Atg6* transgene in the entire fat body (*n*=7). Scale bar: 50 μm.

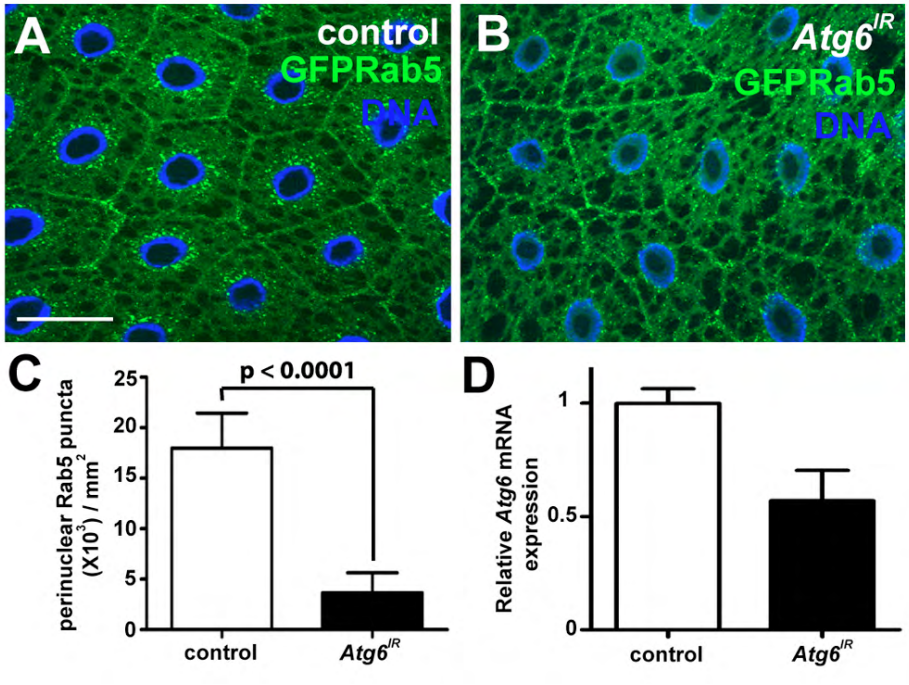

Fig. S2. Loss of *Atg6* leads to defects in Rab5 localization. (**A**) GFP-Rab5 distribution in control fed fat body cells is prominant at the plasma membrane and perinuclear region (*n*=11). (**B**) Fat body cells expressing *Atg6*^{IR} have fewer GFP-Rab5 puncta in the perinuclear region and at the plasma membrane (*n*=13). (**C**) Quantification of GFP-Rab5 puncta in the perinuclear region (2 μm diameter ring surrounding the nucleus). Two tailed *t*-test was used for statistical analysis, and the *P*-value relative to control was 1.48×10^{-8}. (**D**) Graph showing relative *Atg6* mRNA level normalized to *rp49* mRNA in control and *Atg6*^{IR}. Error bars represent s.d. Scale bar: 50 μm.

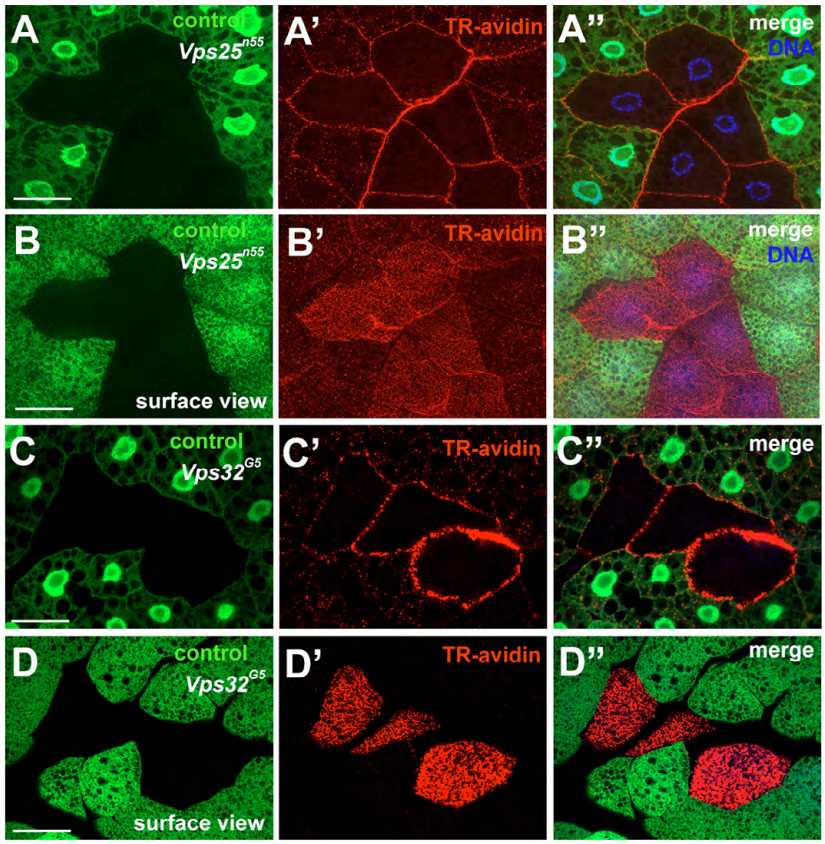

Fig. S3. *Vps25* and *Vps32* mutant cells possess defects in fluid phase endocytosis. (**A-A''**) Texas Red-avidin is endocytosed by control (GFP-positive) fat body cells, but is excluded from *Vps25*^{n55} mutant cells (GFP negative) (*n*=10). (**B-B''**) Surface view of the fat body depicted in A showing accumulation of Texas Red-avidin at the surface of the *Vps25*^{n55} mutant cells but not in control cells. (**C-C''**) Texas Red-avidin is endocytosed by control (GFP-positive) fat body cells, but is excluded from *Vps32*^{G5} mutant cells (GFP negative) (*n*=10). (**D-D''**) Surface view of the fat body depicted in C showing accumulation of Texas Red at the surface of the *Vps32*^{G5}cells but not in control cells. Scale bars: 50 μm.

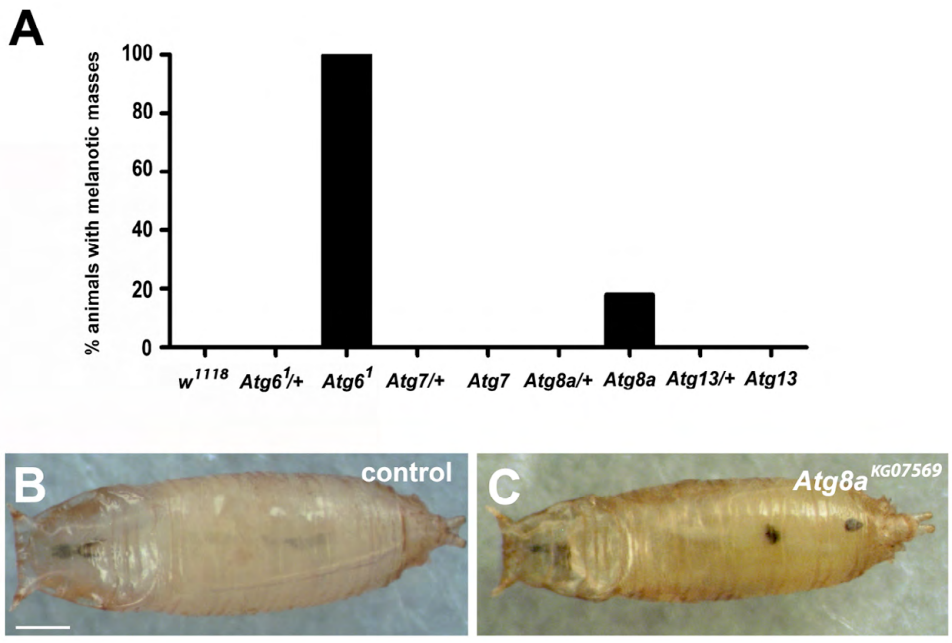

Fig. S4. Mutations in core autophagy genes do not lead to melanotic mass formation. (**A**) Graph showing percentage of larvae/pupae exhibiting melanotic tumor phenotype in w^{1118} (*n*=145) and *Atg6* (*n*=157), *Atg7* (*n*=113), *Atg8a* (*n*=101), *Atg13* (*n*=99) mutant animals. Note that melanotic tumors in *Atg8a* mutant are observed only after pupariation, and that all homozygous *Atg6* mutant larvae possess melanotic tumors. (**B**) Parental control *Atg8a* ^{KG07569}/+ pupae do not have melanotic masses (*n*=94). (**C**) *Atg8a* ^{KG07569}/*Y* (*n*=18/101) pupae contains melanotic masses. Scale bar: 250 µm.

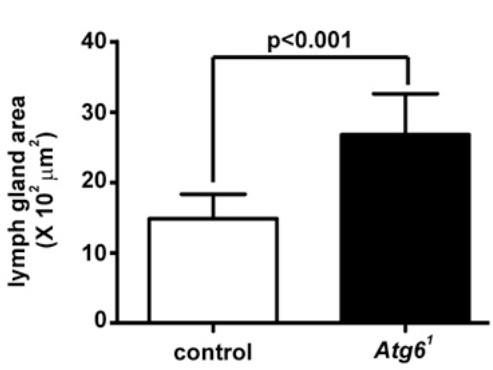

Fig. S5. *Atg6* mutants have enlarged lymph glands. Quantification of lymph gland area in control (*n*=10) and homozygous *Atg6*^{1} (*n*=10) mutants shown in Fig. 7F,G. A two-tailed *t*-test was used for statistical analysis, and the *P*-value relative to control was 6.3×10^{-5}. Error bars represent s.d.